

**DRAG COEFFICIENT REDUCTION OF A 30° YAW ANGLE CUBE
SUBJECTED TO ACTIVE FLOW CONTROL DEVICE BY MEANS OF
NUMERICAL INVESTIGATION**

JEDEDIAH KONG MENG HOI

**This report is submitted
in fulfillment of the requirement for the degree of
Bachelor of Mechanical Engineering (Thermal Fluid)**

Faculty of Mechanical Engineering

UNIVERSITI TEKNIKAL MALAYSIA MELAKA

17 MAY 2017

DECLARATION

I declare that this project report entitled “Drag Coefficient Reduction of a 30° yaw Angle Cube Subjected to Active Flow Control Device by Means of Numerical Investigation” is the result of my own work except as cited in the references

Signature :

Name :

Date :

APPROVAL

I hereby declare that I have read this project report and in my opinion this report is sufficient in terms of scope and quality for the award of the degree of Bachelor of Mechanical Engineering (Thermal Fluid).

Signature :

Name of Supervisor :

Date :

DEDICATION

To my beloved mother and father

ABSTRACT

The concept of three different active flow control devices are applied to a 30° yaw cube is numerically studied by using a commercial software known as ANSYS Fluent at a Reynolds Number of 6.7×10^4 . The percentage of drag reduction on the cube is studied for Moving Surface Boundary Layer Control (MSBC), Synthetic Jet (SJ), and Plasma Actuator (PA). MSBC device is implemented by using two small rotating cylinders located at the windward vertical edges of the cube. SJ device is implemented by setting two small opening of 5mm beside the windward edges which act as a second source of velocity inlet. PA actuating force is done by applying two force term to two areas located beside the windward edges. As for SJ device, the simulation is run with maximum actuation speed of 1m/s, 2m/s, 3m/s, and 4m/s. Simulation for PA device is done with force magnitude of 1mN/m, 2mN/m, 3mN/m, and 4mN/m. The results obtain shows that MSBC device provide greatest average drag coefficient of 28.84% whereas SJ device recorded the lowest drag coefficient reduction of 6.04%. Plasma actuator, being right behind of MSBC device recorded a value of 26.08% reduction of drag coefficient. The result also shows that as active flow control devices are implemented to the cube, region of high vortices formation (which contribute greatly to pressure drag) is significantly reduced.

ABSTRAK

Konsep tiga peranti kawalan aliran aktif yang berbeza digunakan untuk 30° kiub mengoleng yang dikaji dengan menggunakan perisian komersial dikenali sebagai ANSYS Fluent pada nombor Reynolds 6.7×10^4 . Peratusan pengurangan heretan dikaji untuk Kawalan Sempadan Permukaan Bergerak (MSBC), Jet Sintetik (SJ), dan Plasma Penggerak (PA). Peranti MSBC dilaksanakan dengan menggunakan dua silinder kecil berputar yang terletak di sudut hadapan kiub. Peranti SJ dilaksanakan dengan menetapkan dua pembukaan kecil 5mm di sebelah sudut hadapan kiub (menghala kea rah sisi) yang bertindak sebagai sumber kedua masuk halaju. PA penggerak daya dilakukan dengan menggunakan dua kuasa sementara kepada dua kawasan yang terletak di sebelah pembukaat kecil SJ. Bagi peranti SJ, simulasi dijalankan dengan kelajuan maksimum angin pada 1m/ (s,) 2m/s, 3m/ (s,) dan 4m/s. Simulasi untuk peranti PA dilakukan dengan kekuatan magnitud 1mN / m, 2mN / m, 3Mn / m, dan 4mN / m. Keputusan yang diperoleh menunjukkan peranti MSBC mencatatkan peratusan pengurangan heretan tertinggi sebanyak 28.84% manakala peranti SJ merekodkan peratusan pengurangan heretan terendah sebanyak 6.04%. Penggerak plasma pula, mencatatkan peratusan pengurangan sebanyak 26.08%, hanya 2.76% perbezaan pengurangan heretan dibandingkan dengan peranti MSBC. Hasil kajian juga menunjukkan bahawa dengan mengimplementasikan peranti kawalan aliran pada kiub, kawasan pembentukan vorteks tinggi (yang menyumbang besar kepada drag tekanan) dikurangkan dengan ketara.

ACKNOWLEDGEMENT

I would like to express my profound appreciation to my supervisor Dr. Cheng See Yuan for his guidance, advice, as well as support provided to me throughout this research. Although there is slight dispute as well as disagreement among us throughout this research, Dr. still manage to provide a clear path and guidance for me. I sincerely appreciate it.

I would also love to express my gratitude to my friends and lecturers that have provided me with solutions and advices at difficult times faced throughout this research. Your presence and help had always been my motivation to persevere.

Not to forgotten, my family members that have been always supporting me in term of financial and mental, I will not be here without your support.

This research was supported by Universiti Teknikal Malaysia Melaka (UTeM). I thank UTeM for the support in terms of resources provided help completion of this research. Faculty of mechanical engineering (FKM) have been a big contribution for the success of this project. Besides providing computer and software through laboratory located in Fasa B, FKM have also provide seminars, lecturers and lab assistant support to ensure this research is successfully completed.

Last but not least, I would also like to thank other unmentioned parties that have provided guidance throughout the research. I really appreciate your help.

TABLE OF CONTENT

CHAPTER	CONTENT	PAGE
	DECLARATION	ii
	SUPERVISOR'S APPROVAL	iii
	DEDICATION	iv
	ABSTRACT	v
	ABSTRAK	vi
	ACKNOWLEDGEMENT	vii
	TABLE OF CONTENT	viii
	LIST OF TABLES	x
	LIST OF FIGURES	xi
	LIST OF ABBREVIATIONS	xiv
	LIST OF SYMBOLS	xv
CHAPTER 1	INTRODUCTION	1
	1.1 Background	1
	1.2 Problem Statement	3
	1.3 Objective	3
	1.4 Scope Of Project	4
CHAPTER 2	LITERATURE REVIEW	5
	2.1 Bluff-Body Aerodynamics	5
	2.2 Cube Flow	6
	2.3 Synthetic Jet	7
	2.4 Plasma Actuator	10
	2.5 Moving Surface Boundary-Layer Control	13
CHAPTER 3	METHODOLOGY	16
	3.1 Introduction	16
	3.2 Geometry Drawing	18
	3.3 Meshing	19
	3.4 Pre-processing	20

3.5	Post-processing	28
CHAPTER 4	RESULTS AND DISCUSSION	30
4.1	No Flow Control Device	30
4.2	MSBC Device	32
4.3	Synthetic Jet	35
4.4	Plasma Actuator	38
4.5	Grid Independent Test	41
4.6	Data and Comparison	43
4.7	Result Validation	45
4.8	Pressure Fluctuation	46
CHAPTER 5	SUMMARY	48
5.1	Conclusion	48
5.2	Future Work	49
	REFERENCE	50
	LIST OF APPENDIX	54
	APPENDIX	55

LIST OF TABLES

TABLE	TITLE	PAGE
4.5	Details of Mesh used for Grid Independence Test	43
4.6	Data of Drag Coefficient and Percentage Reduction	44

LIST OF FIGURES

FIGURE	TITLE	PAGE
1.1.1	Variation of Drag Force on a Body	1
2.2.1	Instantaneous Velocity Contour with Streamline of B/D=2.0	6
2.2.2	Streamline of Air Flow across a 30° Yawed Cube	7
2.3.1	Schematic Diagram of Synthetic Jet	8
2.4.1	Schematic Diagram of SDBD Plasma Actuator	11
2.4.2	Top View of Plasma Discharge	15
2.5.1	Iso Surface for Natural Case (a) and Controlled Case (b) in the Case of 30° Yaw Angle, Top View	15
2.5.2	Iso Surface for Natural Cases (a) and Controlled Case (b) in the Case of 30° Yaw Angle, Side View	13
3.1.1	Flow Chart of CFD Simulation	17
3.2.1	Geometry of 30° Yaw Cube	18
3.2.2	Location of Synthetic Jet Actuator's Orifice	18
3.3.1	Meshed Product of Cube	19
3.4.1	Location of Rotating Cylinder	21
3.4.2	UDF Code for Synthetic Jet Actuator (clockwise side, x-axis)	22
3.4.3	UDF Code for Synthetic Jet Actuator (clockwise side, y-axis)	22
3.4.4	UDF Code for Synthetic Jet Actuator (counter-clockwise side, x-axis)	23
3.4.5	UDF Code for Synthetic Jet Actuator (counter-clockwise side, y-axis)	23
3.4.6	UDF Code for Plasma Actuator (clockwise side, x-axis)	25
3.4.7	UDF Code for Plasma Actuator (clockwise side, y-axis)	26

3.4.8	UDF Code for Plasma Actuator (counter-clockwise side, x-axis)	27
3.4.9	UDF Code for Plasma Actuator (counter-clockwise side, y-axis)	28
4.1.1	Diagram of Velocity Contour around a Cube with No Active Flow Control Device	30
4.1.2	Diagram of Pressure Contour around a Cube with No Active Flow Control Device	31
4.1.3	Diagram of Velocity Vector around a Cube with No Active Flow Control Device	31
4.1.4	Graph of Drag Coefficient against Time for Simulation with No Flow Control Device	32
4.2.1	Diagram of Velocity Contour around a Cube subjected to MSBC Device	33
4.2.2	Diagram of Pressure Contour around a Cube subjected to MSBC Device	34
4.2.3	Diagram of Velocity Vector around a Cube subjected to MSBC Device	34
4.2.4	Graph of Drag Coefficient against Time for Simulation with MSBC Device Implemented on a Cube	35
4.3.1	Diagram of Velocity Contour around a Cube subjected to SJ	36
4.3.2	Diagram of Pressure Contour around a Cube subjected to SJ	36
4.3.3	Diagram of Velocity Vector around a Cube subjected to SJ	37
4.3.4	Graph of Drag Coefficient against Time for Simulation with SJ Device Implemented on a Cube	37
4.4.1	Diagram of Velocity Contour around a Cube subjected to PA	39
4.4.2	Diagram of Pressure Contour around a Cube subjected to PA	39
4.4.3	Diagram of Velocity Vector around a Cube subjected to PA	40
4.4.4	Graph of Drag Coefficient against Time for Simulation with PA Device Implemented on a Cube	40
4.5.1	Scale of 1.5 cm : 20 mm View for Mesh Generated Around a Cube Used for Grid Independence Test	41

4.5.2	Scale of 1.5 <i>cm</i> : 75 <i>mm</i> View for Mesh Generated Around a Cube Used for Grid Independence Test	42
4.5.3	Scale of 1.5 <i>cm</i> : 175 <i>mm</i> View for Mesh Generated Around a Cube Used for Grid Independence Test	42
4.7.1	Iso-surface of the Time-averaged Streamwise Velocity $U=0$ for No Flow Control Device Case	46
4.8.1	Graph of Pressure Coefficient against Time Step for Synthetic Jet Implemented on a Cube	47

LIST OF ABBEREVATIONS

MSBC	Moving Surface Boundary-Layer Control
SJ	Synthetic Jet
PA	Plasma Actuator
CFD	Computational Fluid Dynamics

LIST OF SYMBOL

f	=	Frequency
D_c	=	Diaphragm Diameter
D_0	=	Orifice Diameter
Δ	=	Amplitude
t	=	Time
$\tilde{u}_0(t)$	=	Fluid leaving Orifice Velocity
C_D	=	Drag Coefficient
F_x	=	Drag Force
A_{ref}	=	Reference Area
F_A	=	Force per Unit Span
$f(t)$	=	Wave Form Function

CHAPTER 1

INTRODUCTION

1.1 BACKGROUND

In general, there are only two distinct types of body, which are streamlined body and bluff body. The major property differentiating these bodies are the type of drag force dominating the body. Viscous drag dominates the drag force of a streamlined body whereas pressure drag dominates the drag force of a bluff body. For a given fixed frontal area and velocity flowing through both types of body, a bluff body will produce higher drag force as compared to a streamline body. This results in many researches done to reduce the drag force for a bluff body. As fluid flows across a bluff body, a large flow separation tends to occur and this will lead to the formation of wake region at the leeward side of the body which prevents pressure from recovering. A larger wake will prevent more pressure recovery from recovering and this will lead to greater pressure drag (Srinivas, 2016). Figure 1.1.1 below shows the variation of drag forces that act on a body.

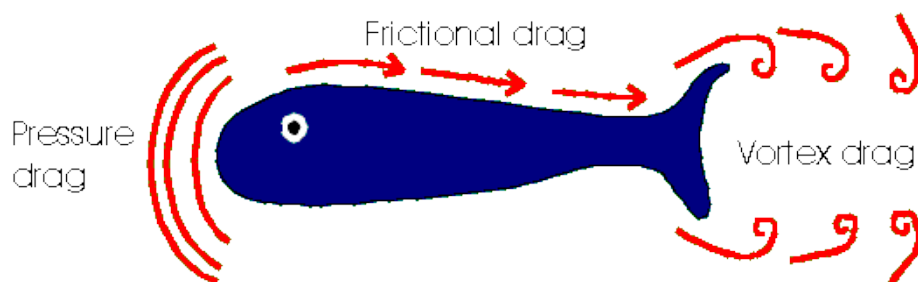


Figure 1.1.1 Variation of Drag Force on a Body (Buchheim J., n.d.)

The modification of wake region is one of the common technique used to reduce the bluff body's drag force. There are two ways to modify the wake region of a body, by using an active flow control device or passive flow control device. Passive control usually utilizes the method of geometry modification and this devices are always operating, regardless of the need. In active flow control method, a device is used to inject extra energy or momentum to the flow. In some cases, active flow control operates only when needed, making it more desirable compared to passive flow control in term of performance. However, additional cost and effort is needed for active flow control. There are three commonly used devices in the application of active flow control which are Synthetic Jet (SJ), Plasma Actuator (PA) and Moving Surface Boundary layer Control (MSBC). These devices have one advantage compared to other device which is it produce zero-net-mass-flux. A research have been done by (Han et. al., 2013) which successfully shown that drag coefficient of a cubical shaped object is reduced with the use of Moving Surface Boundary layer Control (MSBC). On the other hand, a study too have been done by (Pescini et. al., 2016) using plasma actuator to reduce the displacement and momentum thickness of the boundary layer's separated region which in turn reduces the shape factor value.

Although many research have been done independently on using specific active flow control devices, not much attention have been focused on comparing the performance of various flow control devices in drag reduction. This research will be done by using CFD to compare the drag reduction of a 30° yaw cube in a natural flow and various controlled flow techniques.

1.2 PROBLEM STATEMENT

As a flow passes through a cube, the pressure drag dominates the drag force, which means cube is a bluff body. According to a research done by (Xingsi and Siniša, 2013), the use of MSBC technique reduced the drag force of a 30° yawed cube by up to 44%. However, as many research have been done by using individual active flow control device to test the drag reduction of a certain shape, not many research have been done to compare the performance of different active flow control device. In this study, simulation will be done to compare the drag reduction result by using SJ and PA with MSCB on a 30° yawed cube. The positioning for the placement of these two devices will be at the exact same spot at which the MCBS is positioned, which is at the both corners of the windward side of the cube. A fixed angle of 45° actuation from the actuation outlet is implemented for both SJ and PA. The same boundary condition will be used.

1.3 OBJECTIVE

The objectives of this project are:

- 1) To numerically investigate the effect of active flow control devices on flow of a 30° yaw cube.
- 2) To quantify the amount of drag coefficient of a cube subjected to constant wind flow and compare the result with the same cube equipped with Moving Surface Boundary-layer Control (MSBC) device, Synthetic Jet (SJ) and Plasma Actuator (PA).

1.4 SCOPE OF PROJECT

The scopes of this project are:

- 1) Simulating flow around a cube with Reynolds number of 6.7×10^4 .
- 2) Using 4 magnitudes of Synthetic Jet maximum actuation speed which are 1 m/s , 2 m/s , 3 m/s and 4 m/s
- 3) Using 4 magnitudes of Plasma Actuator force value which are 1 mN/m , 2 mN/m , 3 mN/m and 4 mN/m .
- 4) Comparing the drag coefficient reduction around a cube after the cube is equipped with MSBC device, Synthetic Jet, and Plasma Actuator.
- 5) Obtain visualization and compare the flow of air around a 30° yaw cube in natural flow and controlled flow.

CHAPTER 2

LITERATURE REVIEW

2.1 Bluff-Body Aerodynamics

In a research done by Roshko (1993) and Bearman (1997), it have been accurately described that bluff bodies exhibit various major aerodynamic properties such as high pressure drag, large separated flow region, and the existence of vortex shedding. This is caused by the viscous and inviscid flow interaction, which prevent the flow from attaching as it passes through the body. Pressure difference between frontal and leeward faces of the body due to the formation of vortex shedding in the separated region leads to high amount of pressure drag over a long-time average (Sara, 2014). Although vortex shedding is usually associates with two-dimensional body, a research done by Bearman (1977) shows that weaker vortex shedding form may be found in a three-dimensional body. Bearman adds that above some critical Reynolds number, a regular nominal two-dimensional body vortex shedding will display a three dimensional properties through vortex separation, vortex dislocation, looping of vortices, and oblique shedding. As the flow achieves high Reynolds number, numerous three-dimensional motions dominate the wake region. Some of the motions are related to the span wise instabilities of Karman vortices, where others are either related to the smaller-scale to shear layer instability or turbulence flow across the body (Bearman, 1977).

2.2 Cube Flow

In a research done by Ying et. al. (2012), by using Reynolds number of 21400, the aerodynamic patterns of rectangular cylinders with various aspect ratios are determined. From the results obtain, Ying categorized the patterns into three types, namely separated type ($B/D=1.0$ and $B/D=2.0$), intermittently reattached type ($3.0 < B/D < 6.0$) and fully reattached type ($7.0 < B/D < 10.0$). Thus, a cube can be categorize as the same flow as rectangular cylinder with aspect ratio of $B/D=2.0$. Ying also mentioned that the three-dimensional properties of the flow will become more significant as the location from the separation point is further from the leading point.

From Figure 2.2.1 below, there are recirculating vortices generated around the upper and lower surfaces of the wall, with flow separation at the leading edge remain unattached to the wall. Not only that, the vortex generated behind the cross-section is far away from the back surface, resulting in relatively small Strouhal number.

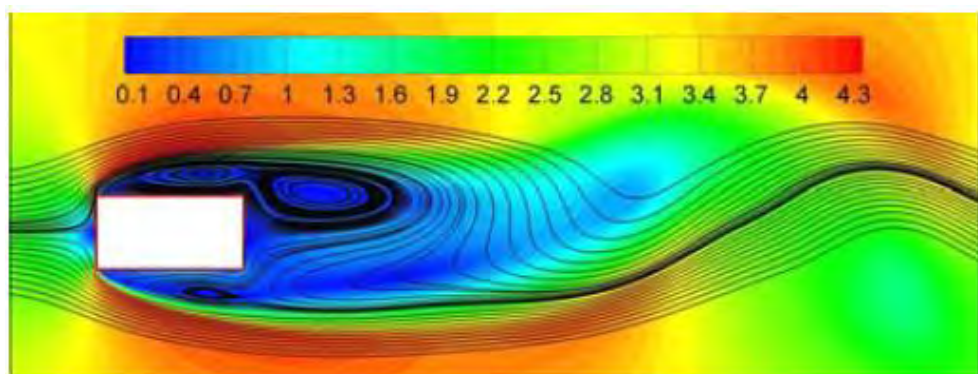


Figure 2.2.1 Instantaneous Velocity Contour with Streamline of $B/D=2.0$ (Ying et. al., 2012)

In another research done by Xingsi and Siniša (2012) on the flow across a 30° yawed cube, based on the streamline flow diagram, we can deduce that the pressure is maximum at the front left edge of the cube. In Figure 2.2.2, as the flow travel through the cube to the right side of the cube, there is a great pressure drop. This happens as the flow starts separating. The difference in pressure at the front of the cube and the side of the cube causes large drag force.

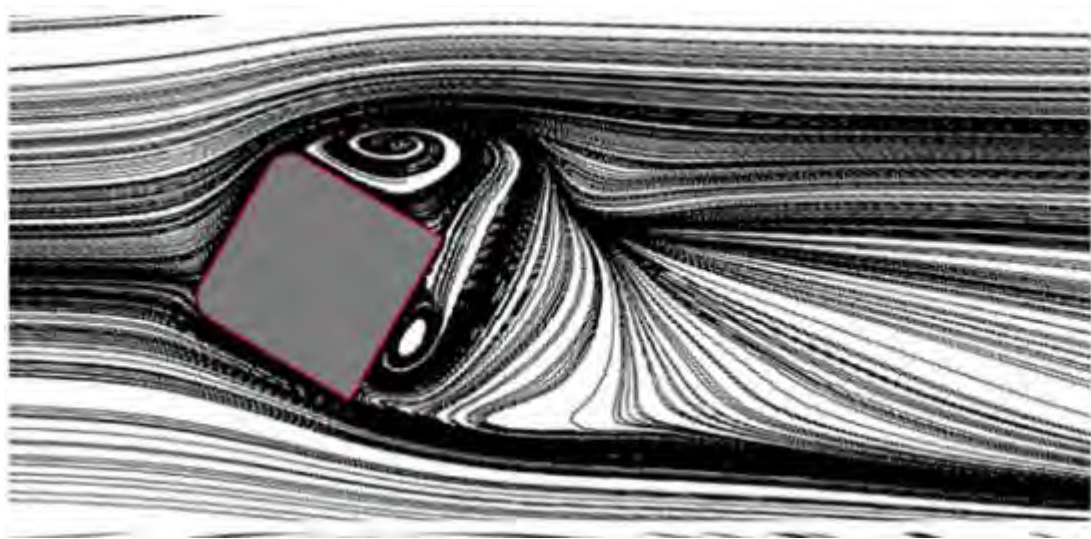


Figure 2.2.2 Streamline of Air Flow across a 30° Yawed Cube (Xingsi and Siniša, 2013)

2.3 Synthetic Jet

Synthetic jet (SJ) is generated by vibrating membrane which is located at the base of an enclosed area. The force generated pushes the air through a circular orifice located at the top of the enclosed area which generates pulsation of air. The SJ actuator is made up of various sections, namely rigid-walled chamber, a round orifice air inlet in the upper surface exposed to outside flow, and an elastic membraned located opposite of the orifice as can be seen in Figure 2.3.1 blow. The working mechanism

of SJ actuator have been discussed by Macovei and Florin (2014). Mocevei and Florin (2014) mentioned two major steps in the working mechanism. Firstly, outer air is sucked into the cavity through the orifice when the membrane moves downward. The second step is when the membrane moves upward, causes the fluid to be discharged through the orifice. Vortex ring will be generated as the fluid discharge through the orifice with sufficient energy. Upon continuous upwards and downwards movement of the membrane, generation of vortices column will occur. The vortices column add momentum to the outer fluid without adding mass flux. Mocevei and Florin (2014) also stated that SJ is available for various application due to its wide range of time and length scale.

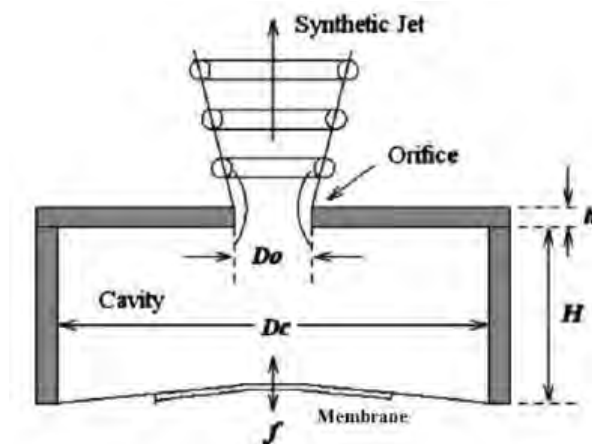


Figure 2.3.1 Schematic Diagram of Synthetic Jet (Macovei and Frunzulica, 2014)

As for the flow separation, it is generally controlled through three working mechanisms. First, additional momentum is injected by the synthetic jet into the ambient freestream flow, adding energy to the retarding boundary layer. Second, high-momentum flow is generated into the boundary layer through continuous successive vortex structures produced by SJ (Zhong et. al., 2007). Third, the detached shear flow or separation bubble becomes unstable due to the oscillation of synthetic jets at

frequencies in a specific range. This causes breaking down of the large-scale flow structure correlated with detached shear flow into smaller-scale flow (Tang et. al., 2013)

The periodic motion of diaphragm in the actuator driven by piezoelectric disc produce an unsteady forcing flow (Glezer & Amitay, 2002), which definitely differ from a steady forcing flow. Although this flow is way more complex as compared to a steady forcing flow, it presents three major advantages: smaller order of power requirement magnitude, possible decoupling of actuators from main propulsive system, and SJ are small-sized, light, and autonomous (Greenblatt & Wygnanski 2000).

According to Arun and Ankit (2015), it is expected that maximum jet velocity affects the jet penetration effect. Thus, taking the same average velocity of uniform profile (steady blowing) and parabolic profile (unsteady blowing), a parabolic profile will have the advantage of having higher maximum velocity at the jet centre. In turn, a parabolic profile jet will be able to penetrate deeper as compared to a uniform profile jet. Arun and Ankit (2015) also stated that while there are backflow along the wake centreline during unsteady forcing flow, the effect is negligible. Not only that, Arun and Ankit (2015) discover that upon taking jet momentum into consideration, the drag coefficient is greatly reduced.

A study have been done by Jeon (2004) by implementing periodic blowing and suction from an orifice on a sphere. The Reynolds number used in this study is 10^5 and this study focuses on reducing drag force by the means of using active flow control device. In this study, the forcing frequency is set in a range of one to thirty times of the vortex-shedding's natural frequency. The results obtained from this study shows that by the implementation of SJ, drag on the sphere was reduced by 50% by using